# Sensitivity of Diagnosed Convective Fluxes to Model Assumptions[1]

CHEE-PONG CHENG AND ROBERT A. HOUZE, JR.

*Department of Atmospheric Sciences, University of Washington, Seattle, 98195*

(Manuscript received 31 July 1979, in final form 5 November 1979)

ABSTRACT

The sensitivity of diagnosed cloud mass and heat fluxes over tropical oceans to assumptions about cumulus-scale updrafts and downdrafts is tested. The ensemble of clouds investigated is the population of precipitating clouds observed in GATE. The basic input to the calculations is radar data. However, a previous paper shows that the same sensitivity is involved in diagnostic calculations based on large-scale heat and moisture budgets.

The assumptions investigated include the relationship between entrainment rate and cloud size, thermodynamic conditions at the base of convective updrafts, thermodynamic properties of entrained air, thermodynamic conditions at the tops of convective downdrafts, and the mass flux profiles in the updrafts and downdrafts. Diagnostic results are most sensitive to the relation between cloud size and entrainment rate and the thermodynamic conditions at the base of the updraft. It is found that assumed mass flux profiles that do not concentrate all of the detrainment from updrafts at cloud top lead to apparently more reasonable heating profiles in the high troposphere. Generally, however, the uncertainty in the diagnostic results that can be attributed to cumulus-scale model assumptions is small, no greater than the uncertainty inherent in the basic data.

## 1. Introduction

In Houze *et al.* (1980, hereafter referred to as H) we developed a set of equations for diagnosing the properties of tropical cloud populations from a radar-observed rainfall spectrum. This diagnostic method is an extension of that developed by Austin and Houze (1973) and Houze and Leary (1976), and we refer to it as the *radar approach*. In H, we showed further that the equations for the radar approach are consistent with those used to diagnose cloud properties from mass, heat and moisture budget data derived from synoptic observations (e.g., Johnson, 1976). We call this latter method the *synoptic approach*.

Both approaches involve the representation of actual clouds by model clouds, and, consequently, the diagnostic results obtained by either approach are model-dependent. In H, we showed that both approaches actually involve the same set of model assumptions, and, using data from GATE[2], we performed a controlled experiment, which showed that similar diagnostic results can be obtained by either approach, provided the arbitrary model assumptions are handled the *same* way in both approaches. However, unless we are further confident that the assumptions are handled *realistically* in the two approaches, we have no assurance that the diagnostic results obtained in either case are accurate. The concern of this paper [as well as that of Leary and Houze (1980)] is to investigate the sensitivity of the diagnostic results to model assumptions.

The model assumptions identified in H are of two types. Some deal with cumulus-scale updrafts and downdrafts, while others deal with the mesoscale air motions associated with precipitating anvil clouds. Anvil clouds and their associated air motions and precipitation are now thought to have been quite important in GATE (Zipser, 1977; Houze, 1977; Zipser and Gautier, 1978; Leary and Houze, 1979a,b; Cheng and Houze, 1979). Johnson (1980) and Leary and Houze (1980) deal extensively with the sensitivity of diagnostic results to the inclusion of anvil air motions in diagnostic models. In the present paper, we consider the sensitivity of diagnostic models to assumptions dealing with the cumulus-scale updrafts and downdrafts.

Several previous studies have also dealt with the sensitivity of diagnostic results to assumptions about the cumulus-scale drafts. For example, Yanai *et al.* (1976) tested differences in results obtained by bulk (Yanai *et al.*, 1973) and spectral (Ogura and Cho, 1973; Nitta, 1975) approaches. These cloud models involved only cumulus-scale updrafts. The cloud models used in the bulk and spectral methods were basically similar, but the bulk approach in-

[1] Contribution Number 516, Department of Atmospheric Sciences, University of Washington.

[2] The Global Atmospheric Research Program's Atlantic Tropical Experiment.

0022-4928/80/040774-10$06.50

volved some extra assumptions concerned with cloud microphysics. The test showed that the two approaches gave similar results, implying that the results of the bulk approach were insensitive to the cloud microphysical assumptions. In our paper, we follow a spectral approach; hence, these cloud microphysical assumptions are not involved.

Nitta (1975) and Esbensen (1975) have tested the sensitivity of diagnostic calculations to assumed thermodynamic conditions at cloud base and found the sensitivity to be significant. In Section 4 of this paper, we further examine the uncertainty associated with cloud-base conditions. Austin and Houze (1973) and Johnson (1977) examined the sensitivity to the shapes of assumed mass flux profiles. The profile shapes are implied by assumptions about detrainment from the sides of the updrafts. Considering extreme cases, Austin and Houze (1973) estimated that the uncertainty associated with these assumptions could be as much as a factor of 2. Johnson (1977), however, found only about a 15–20% difference in the diagnosed mass fluxes for the cases he considered. We examine the sensitivity of diagnosed fluxes to the assumed convective updraft mass flux profiles further in Section 7. Johnson (1976) and Nitta (1977) examined the sensitivity of diagnosed mass and heat fluxes to the inclusion or exclusion of cumulus-scale downdrafts in their assumed cloud models. Inclusion of the downdrafts substantially reduced the diagnosed mass flux by small clouds. In this paper, we do not consider the question of whether convective-scale downdrafts should be included, since this is strongly indicated by Johnson (1976) and Nitta (1977). However, in Section 6, we do examine the sensitivity of diagnosed fluxes to assumptions about the thermodynamic conditions at the downdraft starting level.

Besides reexamining the sensitivity of diagnosed mass and heat fluxes to assumptions regarding cloud-base conditions, updraft mass flux profiles and downdraft starting level conditions, we consider the sensitivity to assumptions regarding the relationship between properties of the air entrained into the convective updrafts and downdrafts (Section 5) and convective downdraft mass flux profiles (Section 7). The assumptions we test in this paper include all of the assumptions regarding cumulus-scale drafts in assumptions (i)–(vii) of H.

All the previous sensitivity tests referred to above used the synoptic approach, except Austin and Houze (1973), who used the radar approach. In this paper, we also use the radar approach. Since in H it was shown that similar diagnostic results are obtained by either approach, the sensitivity to model assumptions shown by one approach should be indicative of the sensitivity of the other approach to the same model assumptions. The choice of one approach or the other to check sensitivity is rather arbitrary. Our method using the radar approach is described below.

## 2. Method

In the controlled experiment of H, two diagnostic calculations were made. A *synoptic control* calculation was made using the synoptic approach. A *radar control* calculation was made using the radar approach. As noted above, the model assumptions were the same in both calculations. The input data for the synoptic control calculation were the mass, heat and moisture budget data of Thompson *et al.* (1979). The radar control calculation used the radar-derived rainfall spectrum of Cheng and Houze (1979) as input. Since the model assumptions were the same in the two calculations and similar results were obtained, either the radar control or the synoptic control calculation can serve as a standard for testing model assumptions.

We choose to use the radar control calculation as a standard, our approach being to alter the assumptions in the radar calculations, recalculate the diagnostic results and compare them with those obtained in the radar control case. That is, we hold the input data constant and vary the model assumptions, whereas in H the model assumptions were held constant and the input data varied. Thus, differences between the diagnostic results obtained previously, in the radar control and synoptic control cases (Figs. 5–10 of H) indicate the uncertainty owing to the different sources of data from which they were derived, while differences between the recalculated radar results and the radar control calculation, obtained in this paper, indicate the magnitude of the uncertainty in the diagnostic results inherent in model assumptions.

## 3. Entrainment

The first model assumption we examine is the function relating convective cell height and entrainment rate [assumption (i) in H]. Two such functions are shown in Fig. 1. The curve labeled "diagnosed" was used in the controlled experiment of H. It is a smoothed version of the curve obtained by assuming that cell top (pressure level $p_T$) was located at the level of zero buoyancy for a given entrainment rate $\lambda$. The smoothing, explained in H, has little effect on our results since we are concerned primarily with clouds with tops above the 600 mb level. The curve labeled "empirical" is a slightly modified version of the entrainment profile used by Austin and Houze (1973), Houze (1973) and Houze and Leary (1976). This curve was chosen to be consistent with laboratory and field studies (cited in Austin and Houze, 1973), which suggest that cumulus clouds with tops near 2 km have entrainment rates $\sim 0.1$ km$^{-1}$, while deep, overshooting

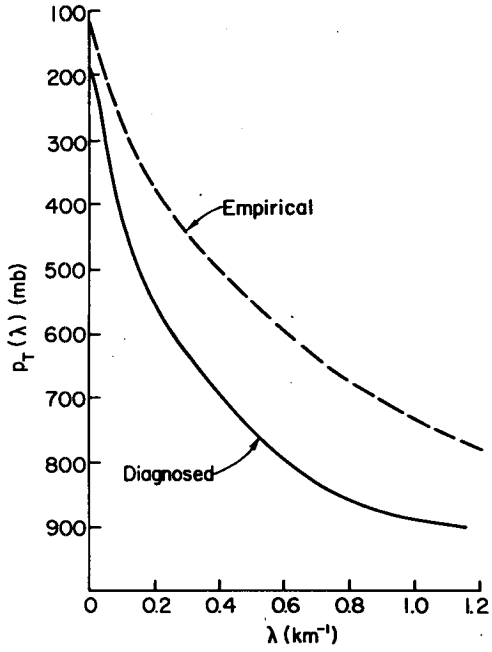


FIG. 1. Functions relating pressure at the tops of convective cells $p_T$ to entrainment rate $\lambda$. "Empirical" curve is adapted from Austin and Houze (1973). "Diagnosed" curve is from Houze *et al.* (1980).

cells ["hot towers" in the terminology of Riehl and Malkus (1958)] have a nearly zero entrainment rate. This empirical curve gives entrainment rates about a factor of 2 greater than those of the diagnosed curve. The difference between these two independently derived curves is probably representative of the inherent uncertainty in the value of the entrainment rate.

To test the sensitivity of diagnosed mass and heat fluxes to this uncertainty, we have recalculated the radar control case of H, with the empirical entrainment curve substituted for the diagnosed entrainment curve (Fig. 2). Use of the larger empirical entrainment rates results in the diagnosis of a convective updraft mass flux ($M_u$) that is larger in the middle and upper troposphere and smaller in the lower troposphere than that obtained in the radar control case (Fig. 2a), while the heat flux by convective updrafts ($H_u$) is smaller at all levels than in the radar control case (Fig. 2b). These changes, associated with the assumed values of the entrainment rate, are significant, being somewhat larger than the data uncertainties indicated by the magnitudes of the differences between the radar control and synoptic control curves (Figs. 6 and 7 of H).

The large change in $M_u$ at middle and upper levels, obtained when the larger empirical entrainment rates are used, can be understood by combining (H2)[3] and (H3) to obtain

$$M_u(z) = (A\tau)^{-1} \int_0^{\lambda_T(z)} \mathcal{M}_B(\lambda) f_u(\lambda,z) d\lambda, \qquad (1)$$

where the notation here, as well as throughout the rest of this paper, is the same as in H. Since there is a one-to-one correspondence of $\lambda$ and cell top height $z_T$ [Eq. (H1)], we can change the variable of integration in (1) to $z_T$ and obtain

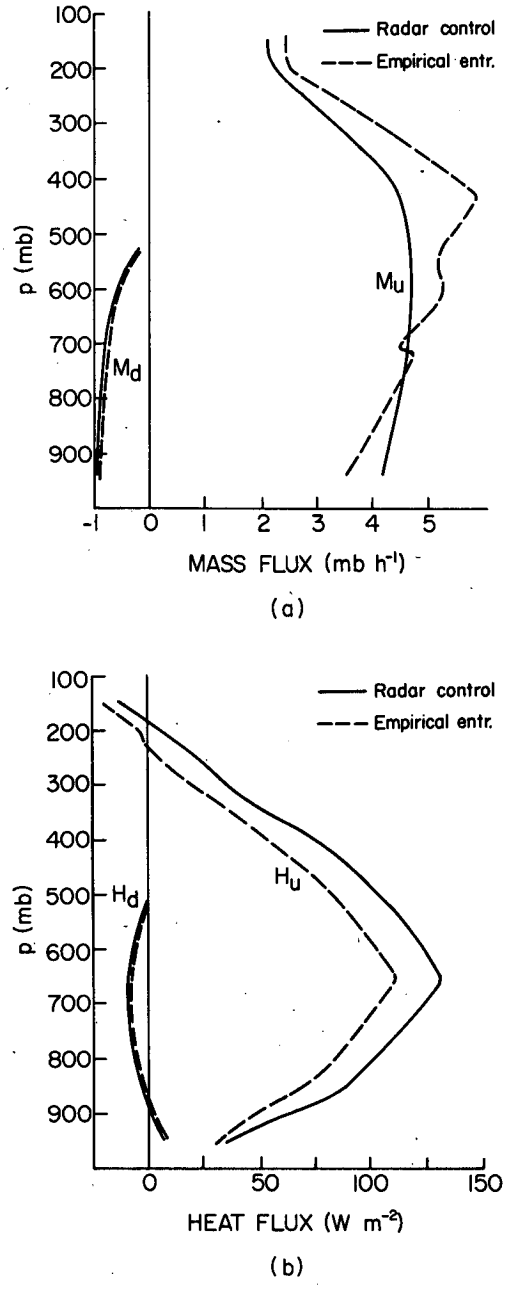


FIG. 2. Mass fluxes (a) and heat fluxes (b) diagnosed in the radar control case and recalculated with the empirical entrainment rate. $M_u$ and $H_u$ refer to convective updrafts; $M_d$ and $H_d$ refer to convective downdrafts.

[3] Equations in H are denoted with the prefix H.

$$M_u(z) = (A\tau)^{-1} \int_{z_T(\lambda=0)}^{z} \mathcal{M}_B[\lambda(z_T)] f_u[\lambda(z_T),z] \frac{d\lambda}{dz_T} dz_T. \quad (2)$$

With the integral in this form, $M_u(z)$ is seen to be the sum of the mass transport in different cloud-size intervals. In a given cloud-size interval, $z_T$ to $z_T + dz_T$, the terms in the integrand of (2) are all affected by changing $\lambda(z_T)$. At middle and upper levels, however, the dominant change is in the mass flux profile $f_u[\lambda(z_T)]$, which, in the controlled experiment of H, has the exponential form

$$f_u[\lambda(z_T),z] = \exp[\lambda(z_T)(z - z_B)]. \quad (3)$$

This profile follows from the assumption in Eq. (H6) of no detrainment except at cloud top. When $\lambda$ is increased, as in changing from the diagnosed to the empirical curve in Fig. 1, the exponential height variation in (3) becomes exaggerated, leading in (2) to the larger values of $M_u(z)$ at middle and upper levels in the recalculated curves of Fig. 2a.

The smaller values of the heat flux $H_u$ obtained when the larger empirical entrainment rates are used (Fig. 2b) results from greater dilution of the convective updrafts, which, according to (H11), reduces the values of $h_u$ and, hence, the factor $[h_u(\lambda,p) - \bar{h}_e(p)]$ in the convective heat flux [Eq. (H59)]. In the heat flux, this reduction is strong enough to lead to smaller values of $H_u$ at all levels even though in middle and upper levels the diagnosed mass flux is increased (Fig. 2a).

Since the diagnostic results are sensitive to the assumed cloud size-entrainment rate relationship, the choice of an appropriate relationship is rather important. Our preference would be for the diagnosed curve in Fig. 1 since this relationship is based on physical reasoning tailored to a particular set of large-scale environmental conditions, and since there is considerable observational uncertainty in the empirical curve.

## 4. Cloud-base conditions for the convective updrafts

The next assumption we examine is the value of moist static energy at cloud base $h_u(\lambda,z_B)$ [assumption (v) of H]. This value is needed to obtain the solution for $h_u(\lambda,z)$ from (H11). In the radar control case, $h_u(\lambda,z_B)$ was determined using Johnson's (1976) assumption of a zero virtual temperature excess at the base of the updraft. For comparison, we recalculated $h_u(\lambda,z)$ using a cloud-base value of $h_u(\lambda,z_B)$ determined by assuming that the air at the base of the updraft was saturated at the temperature of the large-scale environment. The mass and heat fluxes diagnosed using this value of $h_u(\lambda,z)$ are compared to those obtained in the radar control calculation in Fig. 3. Since the value of $h_u(\lambda,z_B)$ in the recalculated case is larger than Johnson's

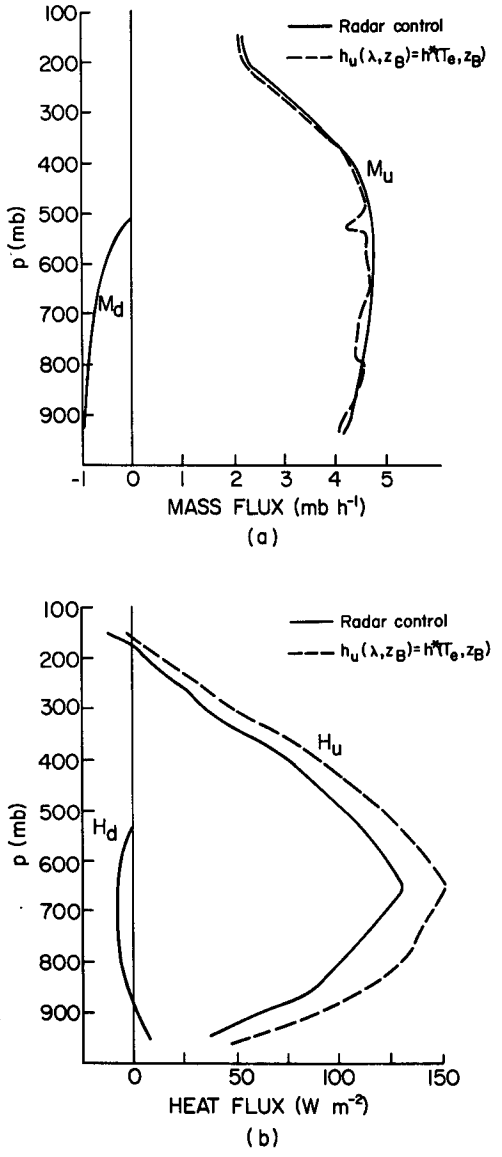


FIG. 3. As in Fig. 2 except that the fluxes have been recalculated under the condition that the moist static energy at the base of the convective updrafts $[h_u(\lambda,z_B)]$ is given by the saturation moist static energy of the large-scale environment $[h^*(T_e,z_B)]$.

value, the recalculated values of $h_u(\lambda,z)$ are larger at all levels than the values obtained in the radar control case. Hence, the convective updraft heat flux $H_u$ is substantially increased throughout the troposphere in the recalculated case (Fig. 3b). The slight difference in the diagnosed updraft mass transports $M_u$ in Fig. 3a comes from the slightly different value of $q_u(\lambda,z)$ [which follows from $h_u(\lambda,z)$ and the condition of saturation in the updraft] in the expression for $I_1(\lambda)$ in (H37). $I_1(\lambda)$, in turn, affects the diagnosis of $\mathcal{M}_B(\lambda)$ according to (H36) or (H74), which ultimately affects the value of $M_u(z)$, according to (1).

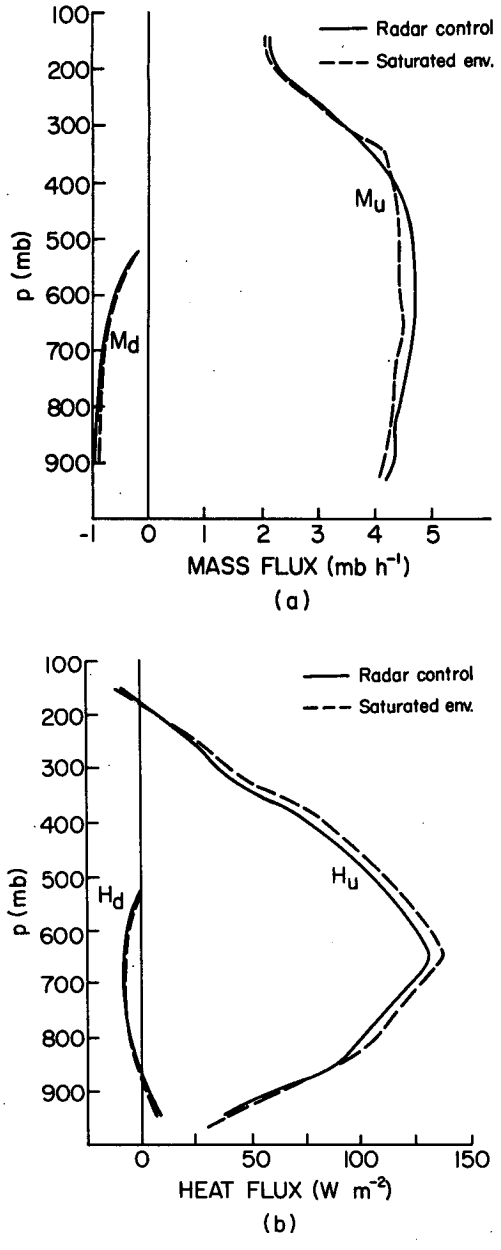


FIG. 4. As in Fig. 2 except that the fluxes have been recalculated for the case in which cells entrain environmental air that is saturated.

The difference between the two calculations of $H_u$ in Fig. 3b indicates that the diagnosed heat flux is quite sensitive to the assumed cloud base conditions. The magnitude of the difference in the two curves is similar to that associated with the uncertainties in the data found in the controlled experiment (Fig. 7 of H). Nitta (1975) and Esbensen (1975) also noted sensitivity to cloud-base thermodynamic conditions. In choosing an appropriate cloud base value of $h_u$, the value used in the controlled experiment [i.e., Johnson's (1976) and Nitta's (1975) choice] appears to be the more reasonable since parcels of air at cloud base had probably not yet reached their level of free convection (i.e., the level at which the temperature of a saturated rising parcel equals the temperature of the large-scale environment).

## 5. Properties of entrained air

In the controlled experiment of H, it was assumed that the air entrained into convective updrafts and downdrafts had the properties of the large-scale environment [assumption (iv) of H]. The validity of this assumption is not obvious *a priori*, as the precipitating convective cells we are concerned with tend to be embedded in large mesoscale rain areas, and there is the possibility that the entrained air is actually part of the surrounding cloud. In this case, the entrained air might be modified environmental air, having, say, a temperature similar to that of the environment but being saturated, or air from neighboring updrafts or downdrafts might be entrained. To test the uncertainty regarding the properties of the entrained air, we recalculated the diagnostic results of the radar control case under the assumption that the air entrained into the convective updrafts and downdrafts was saturated at the temperature of the large-scale environment. The results in Fig. 4 show that the diagnosed mass and heat fluxes are actually not very sensitive to the properties of the entrained air. The difference between the radar control and recalculated curves are smaller than the differences between the radar control and synoptic control curves in Figs. 6 and 7 of H. This insensitivity is probably because we are dealing with precipitating convection, which tends to be deep. Consequently, the entrainment rate is small in any case, so that differences in the properties of the entrained air make little difference in the diagnostic results.

Although the sensitivity to the nature of the entrained air is slight, the behavior of the updraft heat flux $H_u$ is of particular interest *above the 600 mb level*. At those levels, the recalculated $H_u$ (seen in Fig. 4b) slightly exceeds the radar control $H_u$, which, in turn, exceeds the synoptic control $H_u$ (Fig. 7 of H). The synoptic control curve of $H_u$ in Fig. 7 of H was obtained from the total eddy heat flux curve derived as a residual of large-scale terms in a synoptic budget study (Thompson *et al.*, 1979). Below the 600 mb level, the synoptic control curve of $H_u$ in Fig. 7 of H is model-dependent since model downdraft and small-cloud contributions have been removed from the total eddy heat flux of Thompson *et al.* to obtain the updraft contribution $H_u$ to the total. However, the synoptic control curve above 600 mb is not model-dependent since no model downdraft or small cloud effects have been removed from the synoptically derived total heat flux. Therefore, the synoptic control curve at these levels constitutes a stringent

standard for the radar approach calculations to match. Since the recalculated radar curve in Fig. 4b moves away from the synoptic control curve, albeit by a small amount, we conclude that the assumption that updrafts entrain unmodified environment air leads to slightly better diagnostic results than the assumption that the entrained air is saturated at the environment temperature.

### 6. Conditions at downdraft starting level

In the controlled experiment of H, the air at the starting level of the convective downdraft $z_0$ was assumed to be saturated with a temperature excess of zero [assumption ($v$) of H]. This assumption was chosen to be consistent with Johnson (1976). We found, however, that for large cells positive temperature anomalies are computed [using (H21) and (H12)] for the upper part of the downdraft. This result seems unrealistic. Furthermore, it is not clear how the air at the top of the downdraft would have become saturated at the environment temperature. It seems more likely that environmental air entering the cell would be cooled to saturation at its wet bulb temperature, then begin to sink. Therefore, we recomputed the radar control mass and heat fluxes using the condition of saturation at the wet-bulb temperature $T_{we}$ of the large-scale environment. The results are in Fig. 5. Updraft fluxes $M_u$ and $H_u$ are unaffected by this recalculation. The downdraft mass flux $M_d$ is imperceptibly affected. However, the downdraft heat flux $H_d$ (Fig. 5b) is strongly affected, as lower temperatures are computed for all levels of the downdrafts. Negative temperature anomalies are thus obtained at all levels of the downdrafts, giving them a more realistic character, and the heat fluxes are correspondingly lower at all levels. The recalculated heat fluxes do not have the property of being largely negative above the 850 mb level as was the case in the radar control calculation (Fig. 5b) and in previous studies (e.g., Johnson, 1976).

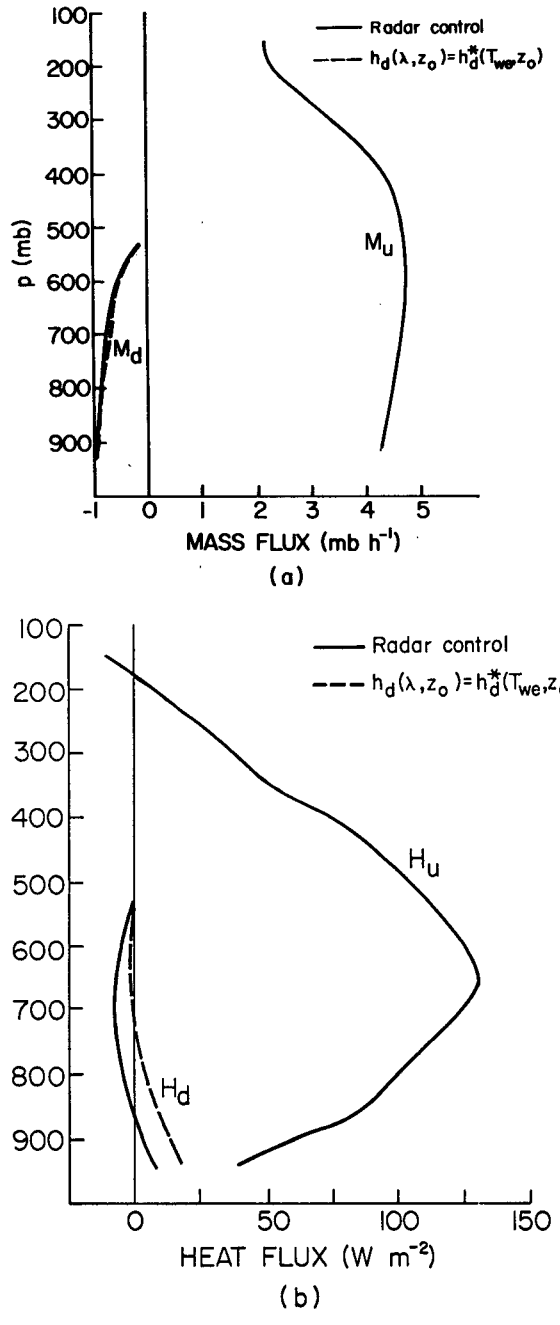


FIG. 5. As in Fig. 2 except that the fluxes have been recalculated under the condition that the moist static energy at the top of the convective downdraft [$h_d(\lambda,z_0)$] is given by the saturation moist static energy calculated at the wet-bulb temperature of the environment [$h^*(T_{we},z_0)$].

### 7. Updraft and downdraft mass flux profiles

The mass flux profile in convective updrafts $f_u[\lambda(z_T),z]$ was assumed to have the exponential form (3) in the controlled experiment of H. The profile for convective downdrafts $f_d[\lambda(z_T),z]$ was taken to be the inverted exponential profile

$$f_d[\lambda(z_T),z] = \exp[-\lambda(z_T)(z - z_0)], \qquad (4)$$

which increases downward from a value of unity at the downdraft starting level $z_0$. As explained in H, these exponential profiles follow from the assumption that detrainment occurs only at the top of the updraft and the bottom of the downdraft.

If detrainment is allowed to occur at the sides of the convective updrafts and downdrafts, various non-exponential profiles are obtained (Austin and Houze, 1973; Johnson, 1977). The updraft profile suggested by Austin and Houze (1973) for use in diagnostic calculations [and used by Houze (1973), and Houze and Leary (1976)] is illustrated in Figs. 6a and 6b. This profile allows most of the detrainment to occur in a layer corresponding to the upper one-fourth of the updraft's height and is expressed mathematically as

$$f_u[\lambda(z_T),z] = \frac{F_u[\lambda(z_T),z]}{F_u[\lambda(z_T),z_B]} . \quad (5)$$

For $z_T \leq 13.8$ km, $F_u(\lambda,z)$ is a number $\leq 1$ given by

$$F_u(\lambda,z) = \begin{cases} \dfrac{2}{2-\lambda}\exp[\lambda(z-\zeta)] \\ \quad -\dfrac{\lambda}{2-\lambda}\exp[2(z-\zeta)], & z \leq \zeta \\ -\left(\dfrac{z-\zeta}{z_T-\zeta}\right)^2 + 1, & \zeta < z \leq z_T \end{cases} \quad (6)$$

where $\zeta$ is the level at which $F_u(\lambda,z)$ has its maximum value of unity. $\zeta$ is located three-fourths of the distance from the base to the top of the updraft, i.e., $\zeta = z_B + 0.75(z_T - z_B)$. Cells observed to extend above 13.8 km are considered to be overshooting. It is assumed, however, that overshooting is a highly transient characteristic and occurs in only a small portion of the convective cloud, so that very little of the updraft's mass flux extends above 13.8 km, which corresponds approximately to the base of the stable layer associated with the tropical tropopause. For overshooting cells ($z_T > 13.8$ km), the profile given by (6) is thus truncated at 13.8 km, as illustrated in Fig. 6c. This profile is expressed mathematically by

$$F_u(\lambda,z) = \begin{cases} \dfrac{2}{2-\lambda}\exp[\lambda(z-\zeta)] - \dfrac{\lambda}{2-\lambda}\exp[2(z-\zeta)], & z \leq \zeta \\ -\left(\dfrac{z-\zeta}{z_T-\zeta}\right)^2 + 1, & \zeta < z \leq 13.8 \text{ km} \\ 0, & \text{if } z > 13.8 \text{ km.} \end{cases} \quad (7)$$

The appearance of $F_u[\lambda(z_T),z_B]$ in the denominator of (5) assures $f_u[\lambda(z_T),z]$ of having a value of one at cloud base, as is required by the definition of $f_u$[Eq. (H3)].

An inverted Austin and Houze updraft profile can be used for the convective downdraft. This profile is given by

$$f_d[\lambda(z_T),z] = \frac{F_d[\lambda(z_T),z]}{F_d[\lambda(z_T),z_0]} , \quad (8)$$

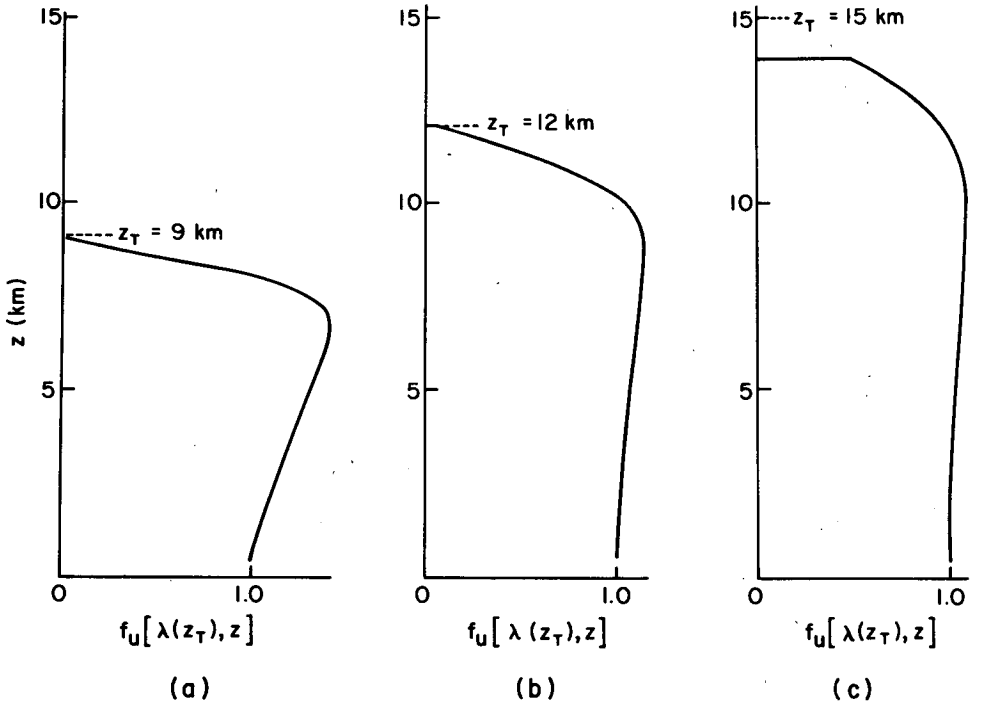


FIG. 6. Mass flux profiles for convective updrafts adapted from Austin and Houze (1973) for cells of height 9 km (a), 12 km (b) and 15 km (c).

where

$$F_d(\lambda,z) = \begin{cases} \dfrac{2}{2+\lambda}\exp[-\lambda(z-z_B)] \\ \quad + \dfrac{\lambda}{2+\lambda}\exp[-2(z-z_B)], & z \leq z_0 \\ 0, & z > z_0. \end{cases} \quad (9)$$

The term $F_d[\lambda(z_T),z_0]$ in the denominator of (8) gives $f_d[\lambda(z_T),z]$ a value of 1 at the downdraft starting level $z_0$. The profile $f_d[\lambda(z_T),z]$ reaches a maximum at the cloud-base level $z_B$. The portion of the profile extending below cloud base is not given here since we do not consider the subcloud layer.

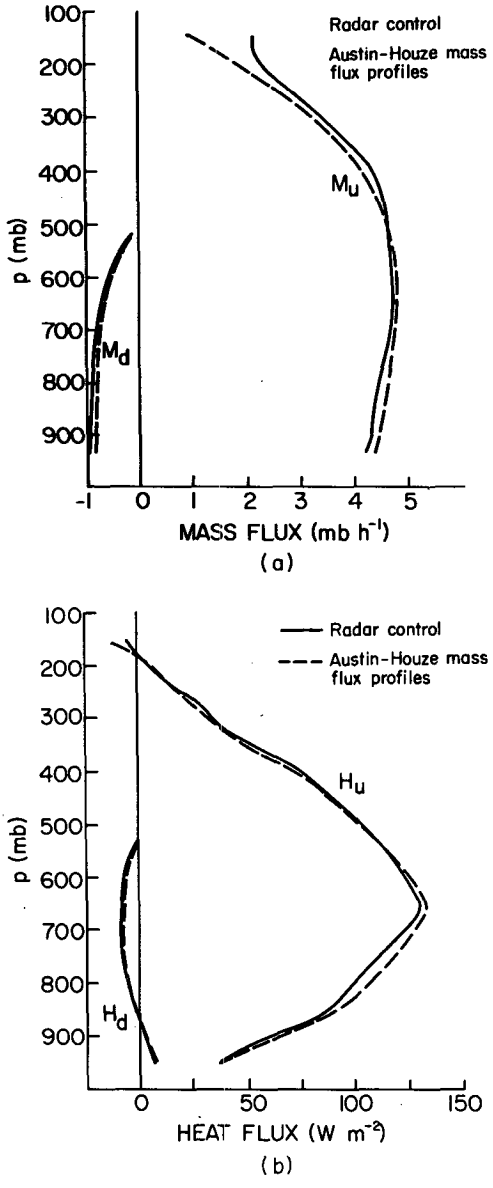


FIG. 7. As in Fig. 2 except that the fluxes have been recalculated using mass flux profiles adapted from Austin and Houze (1973).

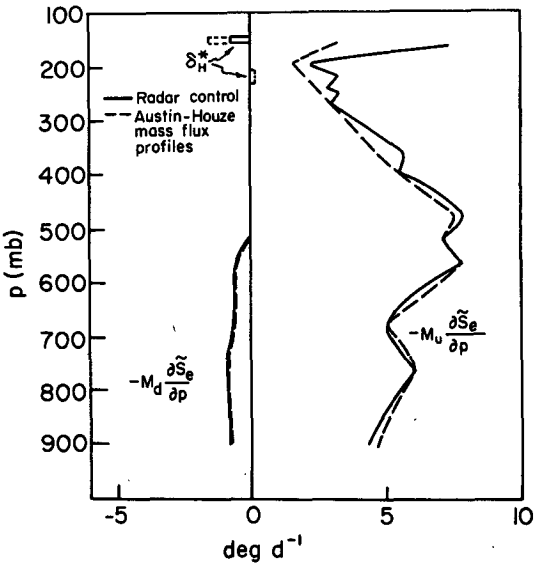


FIG. 8. Contributions to the large-scale heat budget by vertical motions compensating for convective updrafts ($-M_u\partial\tilde{s}_e/\partial p$) and convective downdrafts ($-M_d\partial\tilde{s}_e/\partial p$) and detrainment of moist static energy at cell tops [$\delta_H^* \equiv A^{-1}\tau^{-1}\delta^*(s_u - \tilde{s}_e)$ in the notation of H] diagnosed in the radar control case and recalculated using the mass flux profiles adapted from Austin and Houze (1973).

To test the sensitivity of diagnostic results to the assumed shapes of the profiles $f_u(\lambda,z)$ and $f_d(\lambda,z)$, we recalculated the mass and heat transports of the controlled experiment of H, using the profiles in (6) and (8) in place of (3) and (4). The results are in Fig. 7, where surprisingly little sensitivity to the assumed profiles can be seen [even less than the 15–20% differences found by Johnson (1977)], except for the updraft mass flux $M_u$ at very high altitudes (above 300 mb). At these levels, the recalculated values of $M_u$ are considerably lower than those obtained in the radar control calculation. This result is a consequence of the exponential profile (3) used in the radar control case concentrating the upward mass flux in a given cloud size category at cloud top, while the updraft profile (6) used in the recalculation, has its maximum transport at level $\zeta$, well below cloud top, with a gradual decrease to a mass transport of zero at cloud top.

The sensitivity of the diagnostic results to the different mass transport profiles is further illustrated by Fig. 8, which shows the terms in the sensible heat budget [Eq. (H76)] for the radar control and recalculated cases.

The warming effect of compensating subsidence ($-M_u\partial\tilde{s}_e/\partial_p$), which in the radar control case was

found to be quite large above 300 mb (see discussion in Section 6d of H), is substantially reduced in the recalculated case. This reduction can be associated again with the non-exponential profile (6), which does not concentrate the updraft mass transport at cloud top. The amount of compensating downward motion associated with the upper portions of deep, overshooting cells is lessened when (6) is used.

## 8. Conclusions

From Figs. 2–5 and 7–8, it is concluded that the diagnosis of cloud mass and heat fluxes over tropical oceans is not highly sensitive to assumptions about cumulus-scale updrafts and downdrafts. Generally, the uncertainty associated with these model assumptions is no greater than the uncertainty inherent in the basic data (synoptic and radar).

The assumptions investigated include the relationship between entrainment rate and cloud size, thermodynamic conditions at the base of the convective updrafts, thermodynamic properties of entrained air, thermodynamic conditions at the tops of convective downdrafts, and the mass flux profiles in the updrafts and downdrafts. Of these assumptions, the diagnostic results are most sensitive to the relation between cloud size and entrainment rate and the thermodynamic conditions at the base of the updraft. The magnitude of the uncertainty associated with these two assumptions appears to equal or slightly exceed the uncertainty inherent in the basic data.

From our analysis of the sensitivity of the diagnostic calculations to each of the above assumptions, we conclude that the best set of convective model assumptions for diagnostic calculations is the following:

(i) The cloud-height for a given entrainment rate should be diagnosed as the level of zero buoyancy. Although this assumption is somewhat arbitrary, empirical evidence to the contrary is not strong.

(ii) The thermodynamic conditions at the base of the updraft should be similar or identical to Johnson's (1976) assumption of a zero virtual temperature excess at cloud base since parcels of air at cloud base have probably not yet reached their levels of free convection.

(iii) The air entrained into updrafts and downdrafts should have the same temperature and humidity, or the same moist static energy, as the large-scale environment air. Although the sensitivity to this assumption is small, the assumption of entrainment of air saturated at the environment temperature leads to slightly inferior diagnostic results.

(iv) The air at the top of the convective downdraft $z_0$ should be initially saturated at the wet-bulb temperature of the large-scale environment. The alternative assumption of saturation at the temperature of the environment at level $z_0$ leads to downdrafts with positive temperature excesses, and large negative downdraft heat flux, which seem contrary to most experience with downdrafts.

(v) Mass flux profiles which do not concentrate all of the detrainment from updrafts at cloud top lead to more reasonable heating profiles in the high troposphere.

The absence of extreme sensitivity to convective model assumptions in diagnostic calculations is encouraging for hopes to parameterize the effects of tropical cloud populations in large-scale models. However, this paper has considered only the assumptions associated with *convective-scale* updrafts and downdrafts. One of the major findings of GATE is that *mesoscale* motions associated with anvil clouds and their extensive areas of stratiform rain may also need to be accounted for in the diagnosis and parameterization of cloud processes in the tropics. In Leary and Houze (1980) and Johnson (1980), the sensitivity of diagnostic results to mesoscale motions is examined.

*Acknowledgments.* This work was supported by the Global Atmospheric Research Program, Division of Atmospheric Sciences, National Science Foundation and the GATE Project Office, National Oceanic and Atmospheric Administration, under Grants ATM74-14830 A01 and ATM78-16859.

### REFERENCES

Austin, P. M., and R. A. Houze, Jr., 1973: A technique for computing vertical transports by precipitating cumuli. *J. Atmos. Sci.*, **30**, 400–411.

Cheng, C.-P., and R. A. Houze, Jr., 1979: The distribution of convective and mesoscale precipitation in GATE radar echo patterns. *Mon. Wea. Rev.*, **107**, 1370–1381.

Esbensen, S., 1975: An analysis of subcloud-layer heat and moisture budgets in the western Atlantic trades. *J. Atmos. Sci.*, **32**, 1921–1933.

Houze, R. A., Jr., 1973: A climatological study of vertical transports by cumulus convection. *J. Atmos. Sci.*, **30**, 1112–1123.

——, 1977: Structure and dynamics of a tropical squall-line system. *Mon. Wea. Rev.*, **105**, 1540–1567.

——, and C. A. Leary, 1976: Comparison of convective mass and heat transports in tropical easterly waves computed by two methods. *J. Atmos. Sci.*, **33**, 424–429.

——, C.-P. Cheng, C. A. Leary, and J. F. Gamache, 1980: Diagnosis of cloud mass and heat fluxes from radar and synoptic data. *J. Atmos. Sci.*, **37**, 754–773.

Johnson, R. H., 1976: The role of convective-scale precipitation downdrafts in cumulus and synoptic-scale interactions. *J. Atmos. Sci.*, **33**, 1890–1910.

——, 1977: The effects of cloud detrainment on the diagnosed properties of cumulus populations. *J. Atmos. Sci.*, **34**, 359–366.

——, 1980: A diagnostic model for cloud population properties that includes effects of convective-scale and mesoscale downdrafts. *J. Atmos. Sci.*, **37**, 733–753.

Leary, C. A., and R. A. Houze, Jr., 1979a: Melting and evaporation of hydrometeors in precipitation from the

anvil clouds of deep tropical convection. *J. Atmos. Sci.*, **36**, 669–679.

——, and ——, 1979b: The structure and evolution of convection in a tropical cloud cluster. *J. Atmos. Sci.*, **36**, 437–457.

——, and ——, 1980: The contribution of mesoscale motions to the mass and heat fluxes of an intense convective system. *J. Atmos. Sci.*, **37**, 784–796.

Nitta, R., 1975: Observational determination of cloud mass flux distributions. *J. Atmos. Sci.*, **32**, 73–91.

——, 1977: Response of cumulus updraft and downdraft to GATE A/B-scale motion systems. *J. Atmos. Sci.*, **34**, 1163–1186.

Ogura, Y., and H.-R. Cho, 1973: Diagnostic determination of cumulus cloud populations from observed large-scale variables. *J. Atmos. Sci.*, **30**, 1276–1286.

Riehl, H., and J. S. Malkus, 1958: On the heat balance in the equatorial trough zone. *Geophysica*, **6**, 503–538.

Thompson, R. M., S. W. Payne, E. E. Recker and R. J. Reed, 1979: Structure and properties of synoptic-scale wave disturbances in the intertropical convergence zone of the eastern Atlantic. *J. Atmos. Sci.*, **36**, 53–72.

Yanai, M., S. Esbensen, and J. H. Chu, 1973: Determination of bulk properties of tropical cloud clusters from large-scale heat and moisture budgets. *J. Atmos. Sci.*, **30**, 611–627.

——, J.-H. Chu, T. E. Stark and T. Nitta, 1976: Response of deep and shallow tropical maritime cumuli to large-scale processes. *J. Atmos. Sci.*, **33**, 976–991.

Zipser, E. J., 1977: Mesoscale and convective-scale downdrafts as distinct components of squall-line circulation. *Mon. Wea. Rev.*, **105**, 1568–1589.

——, and C. Gautier, 1978: Mesoscale events within a GATE tropical depression. *Mon. Wea. Rev.*, **106**, 789–805.